



Proceeding Paper

# Mechanistic Insights into the Metabolic Pathways Using High-Resolution Mass Spectrometry and Predictive Models in Pancreatic $\beta$ -Cell Lines ( $\beta$ -TC-6) <sup>†</sup>

Ghada A. Soliman <sup>1,2,\*</sup> , Ye He <sup>2,3</sup> and Rinat Abzalimov <sup>2</sup>

<sup>1</sup> Department of Environmental, Occupational, and Geospatial Health Sciences, Graduate School of Public Health and Health Policy, City University of New York (CUNY), New York, NY 10027, USA

<sup>2</sup> Advanced Science Research Center (ASRC), The Graduate Center, City University of New York, 85 St. Nicholas Terrace, New York, NY 10031, USA; yhe1@gc.cuny.edu (Y.H.); rabzalimov@gc.cuny.edu (R.A.)

<sup>3</sup> The Graduate Center, City University of New York, 365 Fifth Avenue, New York, NY 10016, USA

\* Correspondence: ghada.soliman@sph.cuny.edu

<sup>†</sup> Presented at the 3rd International Electronic Conference on Nutrients, 1–15 November 2023; Available online: <https://iecn2023.sciforum.net/>.

**Abstract:** Objectives: We have previously shown that inhibition of the mTORC1 nutrient-sensing complex by rapamycin and mTORC1/mTORC2 inhibition by either Torin-2 or Rapalink-1 have differential effects on the global untargeted metabolomics in in vivo and in vitro cell culture models. Methods: In this study, we leveraged the mummichog Python algorithm to analyze the high-dimension untargeted metabolomics data to model the biochemical pathways and metabolic networks and predict their functional activity. We used pancreatic beta-cell culture (Beta TC6) and incubated the cells with either Rapalink-1, Rapamycin or the vehicle control for 24 h. Cells were harvested and flash-frozen in liquid nitrogen. Cells were extracted in ethanol, and the supernatant was collected. The untargeted metabolomics was performed using the high-resolution mass spectrometry LC-MS/MS HILIC peak detection of ESI-positive and -negative polarity modes. The data were collected using Bruker's maXis-II ESI-Q-q-TOF coupled to Dionex Ultimate-3000 U(H)PLC system using Sequant ZIC-HILIC 150 × 2.1 mm column (Bruker, Hamburg, Germany). We compared the high-resolution untargeted precision metabolomics (LC-MS/MS) between groups using positive and negative polarity modes to capture both hydrophilic and hydrophobic metabolites. We employed the XCMS plus bioinformatics platform to link mTOR-regulated metabolites to the predicted biological pathways. Statistical significance ( $p < 0.001$ ) was assessed by ANOVA and Ranked order data by Whitney-Cox followed by ad hoc unpaired t-test. Results: The cluster heatmap deconvolution and cloud plot analysis show the differential pattern of metabolites between Rapamycin and Rapalink-treated pancreatic beta cell lines. Mapping the downstream metabolites data onto predictive metabolic pathways and activity networks revealed that the top pathways affected included the pentose phosphate pathway, dopamine and ubiquinol degradation pathways in the ESI-positive polarity mode, and creatine synthesis/glycine degradation and nicotine degradation pathways in the ESI negative polarity mode. Conclusions: The high-resolution untargeted metabolomics can be leveraged as a proxy of the internal exposome yielding high-dimensional data that provide mechanistic insights into metabolic and signaling pathways, and the underlying biology. This approach will have beneficial applications of the internal exposome in determining the optimal precision nutrition pathways for personalized medicine.

**Keywords:** mTORC1; mTORC2; exposome; metabolomics; precision nutrition; high-resolution mass spectrometry

## 1. Background

Precision nutrition entails nutrition approaches tailored to the individual metabolic profile, biological and physiological attributes, social influences, personal circumstances,



**Citation:** Soliman, G.A.; He, Y.; Abzalimov, R. Mechanistic Insights into the Metabolic Pathways Using High-Resolution Mass Spectrometry and Predictive Models in Pancreatic  $\beta$ -Cell Lines ( $\beta$ -TC-6). *Biol. Life Sci. Forum* **2023**, *29*, 16. <https://doi.org/10.3390/IECN2023-15878>

Academic Editor: Francisco José Perez

Published: 7 November 2023



**Copyright:** © 2023 by the authors. Licensee MDPI, Basel, Switzerland. This article is an open access article distributed under the terms and conditions of the Creative Commons Attribution (CC BY) license (<https://creativecommons.org/licenses/by/4.0/>).

and environmental exposures. Achieving such a goal requires system science approaches and an understanding of the mechanistic signaling pathways and networks governing nutrient metabolism. One of the central regulators of metabolic pathways is the mechanistic Target of the Rapamycin (mTOR) protein, which functions as a critical node to regulate carbohydrate, fat, and protein metabolism (synthesis and catabolism). mTOR kinase assembles two functionally distinct and mutually exclusive complexes termed mTORC1 and mTORC2 [1,2]. The Raptor subunit binds the mTOR kinase to form mTORC1—which is activated by Rheb at the lysosomal membrane—to regulate cell metabolism in response to nutrients and growth factors. On the other hand, Rictor facilitates the mTORC2 localization to the plasma membrane, together with mLST8, to scaffold the mSin1 subunit to control glucose homeostasis and cell growth.

In this study, we chemically knocked down mTOR complexes with drugs, including Rapamycin (which mainly inhibits mTORC1) and RapaLink-1 (which inhibits both mTORC1 and mTORC2) to determine the differences between mTORC1 and mTORC2 in their signaling cascade to gain mechanistic insights into the metabolic pathways that govern nutrient metabolism. We applied high-dimension untargeted metabolomics as a proxy of the internal exposome, the totality of exposures across the lifespan, to provide a readout of the differential mechanistic pathways between mTORC1 and mTORC2. Untargeted metabolomics systematically identifies small-molecule metabolites that are affected by the exposome and manifested by biochemical responses and molecular alterations.

## 2. Objectives

We have previously shown that inhibition of the mTORC1 nutrient-sensing complex by Rapamycin and mTORC1/mTORC2 inhibition via either Torin-2 or RapaLink-1 have differential effects on the global untargeted metabolomics in vitro cell culture models [3]. In this proof-of-concept study, we leveraged the mummichog Python algorithm to analyze the high-dimension untargeted metabolomics data for modeling the biochemical pathways and metabolic networks, and predicting their functional activity using the XCMS Plus bioinformatics platform [4,5].

## 3. Methods

We used pancreatic beta-cell culture (Beta TC6), which secretes insulin in response to glucose, and incubated the cells with either (1) RapaLink-1, (2) Rapamycin or (3) control for 24 h. Cells were harvested and flash-frozen in liquid nitrogen. Cells were extracted in ethanol, and the supernatant was collected to be analyzed by a high-resolution mass-spectrometry-based approach (ESI-LC-MS/MS). Both positive and negative ionization modes in ESI-LC-MS/MS were used for untargeted screening and differential analysis of metabolites under various treatment conditions. The data were collected employing Bruker's maXis-II ESI-Q-q-TOF coupled to the Dionex Ultimate-3000 U(H)PLC system using Sequant ZIC-HILIC 150 × 2.1 mm column (Bruker, Hamburg, Germany). Using the mummichog Python algorithm, we employed the XCMS plus bioinformatics platform to link mTOR-regulated metabolites to the predicted biological pathways [4–6]. Metabolites were identified by searching the BioCys database. A multi-group analysis by ANOVA was performed to compare and determine the significant differences between RapaLink-1, Rapamycin, and the control groups. If a statistical significance was determined by ANOVA, we performed a protected pair-wise analysis of samples incubated with either Rapamycin or RapaLink. Statistical significance ( $p < 0.001$ ) was assessed via ranked order data by Whitney-Cox followed by an ad hoc unpaired t-test.

## 4. Results

The principal component analysis (PCA) revealed that each group clustered into at least two components with distinct metabolite signatures (Figures 1A and 2C,D). The cluster heatmap deconvolution (Figure 1B) and cloud plot (Figure 2AB) analysis show the differential pattern of metabolites between Rapamycin and RapaLink-treated pancreatic

beta cell lines. In the cloud plots (Figure 2A,B), the features in green color showed increased metabolites and features in red revealed decreased metabolites in the positive (55 features  $p < 0.001$ ) and negative modes of ionization (344 features  $p < 0.01$ ). Pathway and network analyses showed that mTOR-centered pathways and networks were differentially altered with RapaLink versus Rapamycin. The metabolic pathways and activity network analysis revealed that the top pathways affected included the pentose phosphate pathway, dopamine and ubiquinol degradation pathways in the ESI-positive polarity mode of sample ionization (Table 1), and creatine synthesis/glycine degradation and nicotine degradation pathways in the ESI-negative polarity mode (Table 2).

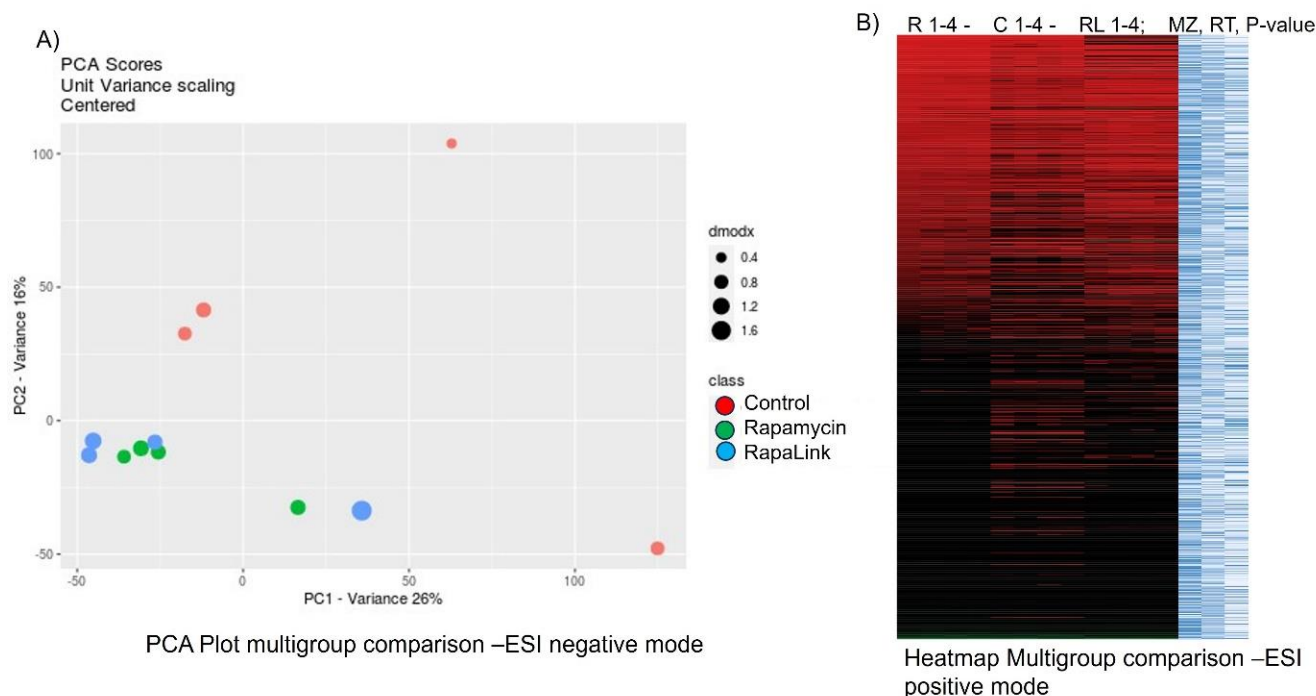


**Figure 1.** Principal component analysis (PCA) and heatmap visualization tools to compare the treatment groups. Pancreatic beta cell lines ( $\beta$ -TC-6) were incubated with either RapaLink, Rapamycin, or control for 24 h. Cells were harvested, flush-frozen, extracted and analyzed using an ESI-LC-MS/MS spectrometry-based approach. The data were collected and analyzed using the XCMS-Plus bioinformatics platform. (A) Principal component analysis (PCA) clusters of the treatment groups. (B) Heatmap visualization of the comparison of the untargeted metabolomics data.

**Table 1.** Dysregulated metabolic pathways comparison between the effects of mTORC1 inhibitor (Rapamycin) and mTORC1/mTORC2 inhibitor (RapaLink-1) in ESI-positive mode. Top pathways are listed below.

Pathways	Overlap_Size	Pathway_Size	$p$ -Value (raw)	$p$ -Value
Pentose phosphate pathway (non-oxidative branch)	2	3	0.023334	0.0
Dopamine degradation	2	7	0.12893	0.00004
Ubiquinol-8-biosynthesis (eukaryotic)	2	11	0.2682	0.00074
Arsenate detoxification I (glutaredoxin)	1	4	0.32129	1

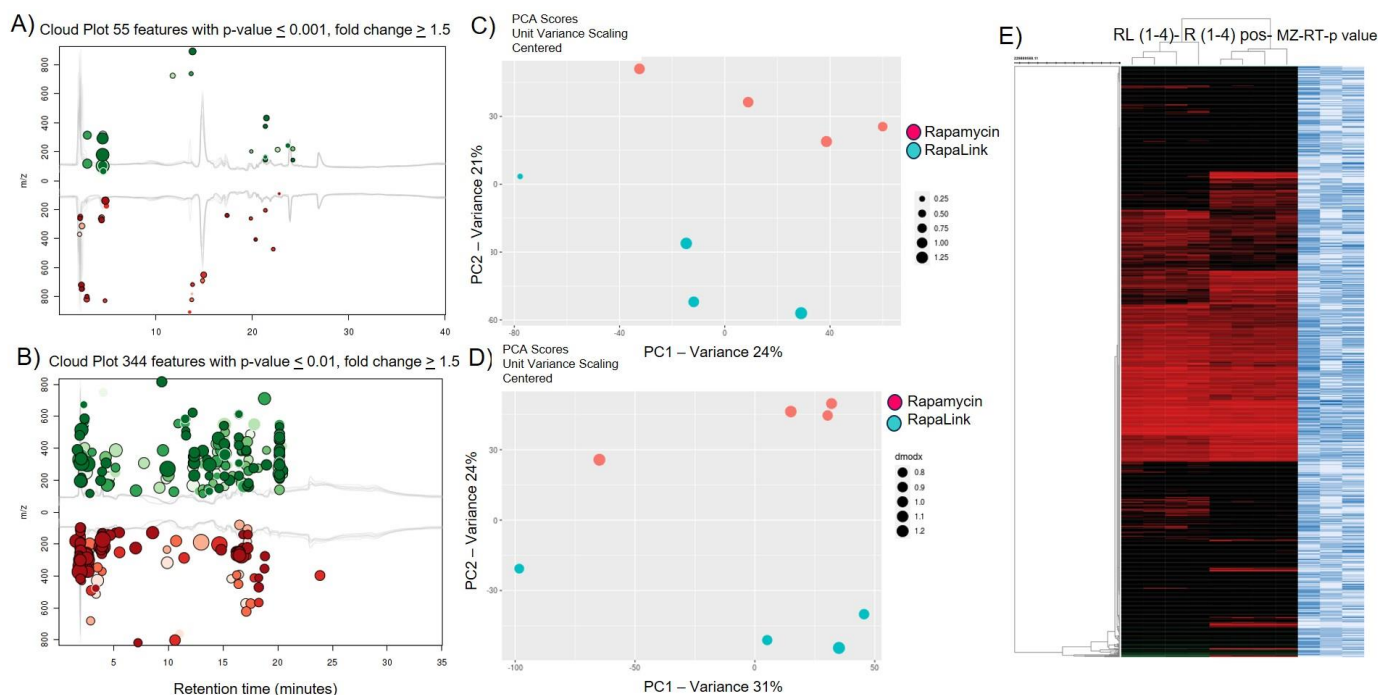


**Figure 2.** Visualization of data by cloud plot, PCA cluster, and heatmap of the differences of the untargeted metabolomics between the effects of mTORC1 inhibitor (Rapamycin) and mTORC1/mTORC2 inhibitor (RapaLink-1) on pancreatic cell lines ( $\beta$ -TC-6) in the ESI-positive and negative modes. Cells were incubated with either Rapalink, Rapamycin or control cells were harvested and analyzed by ESI-LC-MS/MS, followed by bioinformatics analysis using the XCMS-Plus platform. (A) Cloud plot of the comparison between RapaLink and Rapa incubation, showing (A) 55 features in the ESI-positive mode, (B) 344 features with a  $p$ -value  $\leq 0.001$ , and fold change  $\geq 1.5$ . (C) Principal component analysis (PCA) between RapaLink and Rapamycin in ESI-positive mode and (D) ESI-negative mode, respectively. (E) Heatmap of all the features in the global untargeted metabolomics dataset comparison between RapaLink-versus Rapamycin-treated pancreatic beta cells ( $\beta$ -TC-6).

**Table 2.** Dysregulated metabolic pathways comparison between the effects of mTORC1 inhibitor (Rapamycin) and mTORC1/mTORC2 inhibitor (RapaLink-1) in ESI-negative mode. Top pathways are listed below.

Pathways	Overlap_Size	Pathway_Size	$p$ -Value (raw)	$p$ -Value
Nicotine degradation II	4	10	0.0587	0.00289
Phospholipases	2	2	0.02513	0.0053
Glycine degradation (creatine biosynthesis)	3	7	0.08438	0.0058
Creatine biosynthesis	3	8	0.11986	0.00875
D-myo-inositol (3,4,5,6)-tetrakisphosphate biosynthesis	2	3	0.06755	0.01111
D-myo-inositol (1,3,4)-trisphosphate biosynthesis	2	3	0.06755	0.0111
Glutathione biosynthesis	2	3	0.06755	0.0111
1D-myo-inositol hexakisphosphate biosynthesis II (mammalian)	2	4	0.12123	0.02083
L-dopachrome biosynthesis	2	4	0.12123	0.02083
tRNA charging pathway	3	12	0.29586	0.03833

## 5. Conclusions

High-resolution untargeted metabolomics can be leveraged as a proxy of the internal exposome to determine altered metabolites, yielding high-dimensional data that provide plausible mechanistic insights into metabolic and signaling pathways and the underlying biology. This approach will have beneficial applications of the internal exposome in determining the optimal precision nutrition pathways for personalized medicine.

**Author Contributions:** Conceptualization, G.A.S., Y.H. and R.A.; methodology, G.A.S., Y.H. and R.A.; software G.A.S., Y.H. and R.A.; validation, G.A.S., Y.H. and R.A.; formal analysis, G.A.S.; investigation, G.A.S. and Y.H.; resources, G.A.S., Y.H. and R.A.; data curation, G.A.S.; writing—original draft preparation, G.A.S.; writing—review and editing, G.A.S., Y.H. and R.A.; visualization, G.A.S. and Y.H.; project administration, G.A.S.; funding acquisition, G.A.S., Y.H. and R.A. All authors have read and agreed to the published version of the manuscript.

**Funding:** This study is funded by PSC-CUNY Grant 66082-00 54 and the City University of New York, GC Advanced Science Research Center Seed Grant Award # 95649-00-01. XCMS Plus is a platform for analyzing untargeted metabolomics with an integrated METLIN in silico fragmentation tandem MS database [7].

**Institutional Review Board Statement:** Not applicable.

**Informed Consent Statement:** Not applicable.

**Data Availability Statement:** Data will be available upon written request.

**Conflicts of Interest:** The authors declare no conflict of interest.

## References

1. Battaglioni, S.; Benjamin, D.; Walchli, M.; Maier, T.; Hall, M.N. mTOR substrate phosphorylation in growth control. *Cell* **2022**, *185*, 1814–1836. [[CrossRef](#)]
2. Soliman, G.A. The role of the mechanistic target of rapamycin (mTOR) complexes signaling in the immune responses. *Nutrients* **2013**, *5*, 2231–2257. [[CrossRef](#)] [[PubMed](#)]
3. Soliman, G.A.; Abzalimov, R.R.; He, Y. mTORC1 and mTORC2 Complexes Regulate the Untargeted Metabolomics and Amino Acid Metabolites Profile through Mitochondrial Bioenergetic Functions in Pancreatic Beta Cells. *Nutrients* **2022**, *14*, 3022. [[CrossRef](#)]
4. Domingo-Almenara, X.; Siuzdak, G. Metabolomics Data Processing Using XCMS. *Methods Mol. Biol.* **2020**, *2104*, 11–24. [[PubMed](#)]
5. Domingo-Almenara, X.; Montenegro-Burke, J.R.; Ivanisevic, J.; Thomas, A.; Sidibe, J.; Teav, T.; Guijas, C.; Aisporna, A.E.; Rinehart, D.; Hoang, L.; et al. XCMS-MRM and METLIN-MRM: A cloud library and public resource for targeted analysis of small molecules. *Nat. Methods* **2018**, *15*, 681–684. [[CrossRef](#)] [[PubMed](#)]
6. Gowda, H.; Ivanisevic, J.; Johnson, C.H.; Kurczy, M.E.; Benton, H.P.; Rinehart, D.; Nguyen, T.; Ray, J.; Kuehl, J.; Arevalo, B.; et al. Interactive XCMS Online: Simplifying advanced metabolomic data processing and subsequent statistical analyses. *Anal. Chem.* **2014**, *86*, 6931–6939. [[CrossRef](#)] [[PubMed](#)]
7. Huan, T.; Forsberg, E.M.; Rinehart, D.; Johnson, C.H.; Ivanisevic, J.; Benton, H.P.; Fang, M.; Aisporna, A.; Hilmers, B.; Poole, F.L.; et al. Systems biology guided by XCMS Online metabolomics. *Nat. Methods* **2017**, *14*, 461–462. [[CrossRef](#)] [[PubMed](#)]

**Disclaimer/Publisher's Note:** The statements, opinions and data contained in all publications are solely those of the individual author(s) and contributor(s) and not of MDPI and/or the editor(s). MDPI and/or the editor(s) disclaim responsibility for any injury to people or property resulting from any ideas, methods, instructions or products referred to in the content.